Vol. 190, No. 14

Biochemical and Mutational Analyses of AcuA, the Acetyltransferase Enzyme That Controls the Activity of the Acetyl Coenzyme A Synthetase (AcsA) in *Bacillus subtilis*[▽][§]

Jeffrey G. Gardner and Jorge C. Escalante-Semerena*

Department of Bacteriology, University of Wisconsin, Madison, Wisconsin

The *acuABC* genes of *Bacillus subtilis* comprise a putative posttranslational modification system. The AcuA protein is a member of the Gcn5-related *N*-acetyltransferase (GNAT) superfamily, the AcuC protein is a class I histone deacetylase, and the role of the AcuB protein is not known. AcuA controls the activity of acetyl coenzyme A synthetase (AcsA; EC 6.2.1.1) in this bacterium by acetylating residue Lys549. Here we report the kinetic analysis of wild-type and variant AcuA proteins. We contrived a genetic scheme for the identification of AcuA residues critical for activity. Changes at residues H177 and G187 completely inactivated AcuA and led to its rapid turnover. Changes at residues R42 and T169 were less severe. In vitro assay conditions were optimized, and an effective means of inactivating the enzyme was found. The basic kinetic parameters of wild-type and variant AcuA proteins were obtained and compared to those of eukaryotic GNATs. Insights into how the isolated mutations may exert their deleterious effect were investigated by using the crystal structure of an AcuA homolog.

Protein acetylation is a form of posttranslational modification that allows cells to rapidly alter cellular processes in response to a changing environment (14). Acetyltransferase enzymes (referred to as Gcn5-type *N*-acetyltransferases, or GNATs) in eukaryotic cells responsible for some of these modifications have been extensively studied within the context of the control of gene expression. GNATs modulate the acetylation state of histones facilitating transcription (hyperacetylated histones) or gene silencing (hypoacetylated histones) (4, 11–14, 21). GNATs use acetyl coenzyme A (Ac-CoA) as the donor of acetyl groups to modify ε-amino groups of lysyl residues in histone tails. In eukaryotes, GNATs act on different protein substrates and small molecules (1, 7, 10, 15, 16, 24, 25). In contrast, there are only two described examples of prokaryotic metabolic enzymes under GNAT control. The protein acetyltransferase (Pat) enzyme of *Salmonella enterica* and the AcuA enzyme of *Bacillus subtilis* (AcuA$_{Bs}$) control the activity of the central metabolism enzyme Ac-CoA synthetase (AcsA) (5, 18), and in the case of Pat, the enzyme also controls the activity of propionyl-CoA synthetase (6, 19).

Together with protein deacylases, Pat and AcuA comprise the protein acylation/deacylation system of posttranslational modification that helps the cell maintain CoA homeostasis during growth on acetate or propionate (5, 17, 20) (Fig. 1). To date, the kinetic characterization and mutational analyses of the Pat or AcuA enzyme have not been reported.

To advance our understanding of the function of the bacterial AcuA enzyme, we isolated variants of AcuA that com-

pletely or partially lacked activity, quantified the effect of the mutations using an in vitro activity assay, and compared the kinetic parameters of the variant proteins to those of the wild-type protein. The functionality of AcuA variants was also assessed in vivo using strains of *S. enterica* carrying a null allele of the *pat* gene in the chromosome.

Residues critical to AcuA$_{Bs}$ function. We took a genetic approach to the identification of residues that were critical to AcuA$_{Bs}$ function. For this purpose, we took advantage of the fact that the growth of an *S. enterica pat* strain on low acetate (10 mM) is arrested when the AcuA protein is overproduced (5). We introduced single-base mutations into *acuA$^+$* (carried by plasmid pACUA1) using the XL1-Red *Escherichia coli* mutator strain (Stratagene). The strain carrying plasmid pACUA1 was grown as per the manufacturer's instructions. Plasmid DNA was isolated from the mutator strain twice at 24-h intervals, and DNA was transformed into *S. enterica* strain JE6861 [*metE205 ara-9 pat1*::Tn*10*d(*tet$^+$*)] and plated onto no-carbon E (NCE) medium containing acetate (10 mM) and arabinose (500 μM to induce *acuA* expression), with selection for growth. Cells from colonies growing on the selective medium were patched on LB agar plates containing ampicillin (Amp) and were replica printed onto plates with NCE plus acetate plus arabinose plus Amp to assess their ability to grow on acetate. Under these conditions, cell growth implied either the lack of *acuA* expression or the synthesis of AcuA variant proteins with various levels of enzymatic activity. Cells that grew on acetate were inoculated into 2 ml of LB plus Amp and grown overnight. Plasmid DNA was recovered from LB agar- and Amp-grown cells, the *acuA* allele was cut from the plasmid using the restriction enzymes EcoRI and HindIII, and the fragment was recloned into plasmid pBAD30 cut with the same enzymes. Reconstructed plasmids were electroporated into strain JE6861 [*metE205 ara-9 pat1*::Tn*10*d(*tet$^+$*)], with selection for Amp^r cells, and growth on NCE medium containing acetate

---
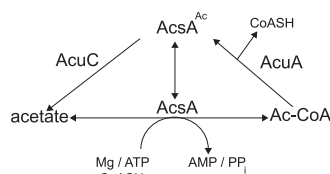
FIG. 1. Posttranslational control of Ac-CoA synthetase activity by the AcuA$_{Bs}$ (acetyltransferase) and AcuC$_{Bs}$ (deacetylase). AcuA uses Ac-CoA to acetylate (inactivate) AcsA. AcuC deacetylates (activates) acetylated AcsA (AcsA^{Ac}), restoring the ability of the Acs enzyme to convert acetate to Ac-CoA. CoASH, free CoA.
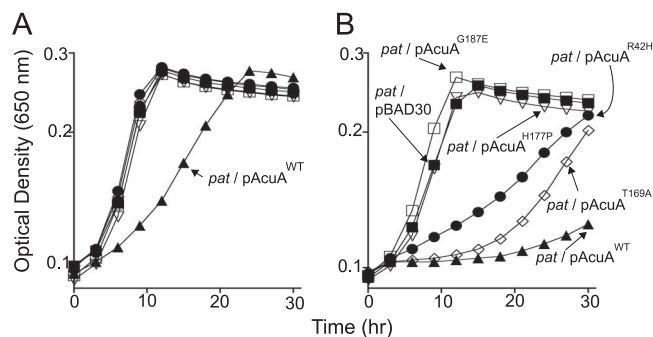

FIG. 2. In vivo assessment of AcuA^{WT} and variant AcuA proteins. All growth experiments were performed at least three times, and each time they were performed in triplicate. In all experiments, the standard deviation was ≤0.5. The size of the symbols obscures the error bars, but they are included in the figure. NCE minimal medium (2) containing acetate (10 mM) as a carbon and energy source was used for these experiments. (A) Behavior of the strains in the absence of L-(+)-arabinose, the inducer used to trigger the synthesis of AcuA proteins. (B) Behavior of the same strains in the presence of 500 μM L-(+)-arabinose in the medium. Filled squares, *pat*/pBAD30 strain (empty vector control); filled triangles, *pat*/pAcuA^{WT} strain; open squares, *pat*/pAcuA^{G187E} strain; open inverted triangles, *pat*/pAcuA^{H177P} strain; circles, *pat*/pAcuA^{R42H} strain; diamonds, *pat*/pAcuA^{T169A} strain. For a complete description of the strain and plasmid genotypes, see Table S2 in the supplemental material. Details of the construction of plasmids and strains, the growth conditions, and medium supplements are described in the supplemental material.

and arabinose was reassessed. Plasmid DNA was isolated from Amp^r cells that grew on acetate in the presence of arabinose, and the *acuA* alleles from these plasmids were sequenced.

The growth behavior of strain JE6861 carrying mutant alleles of *acuA* is shown in Fig. 2. Overproduction of the variant proteins AcuA^{G187E} and AcuA^{H177P} did not affect the growth of the strain on acetate, suggesting that changes at residues G187 and H177 completely eliminated AcuA activity or resulted in a level of activity that was too low to affect growth on acetate. Two other AcuA variant proteins with changes at position R42 (AcuA^{R42H}) or T169 (AcuA^{T169A}) retained some activity, as shown by the intermediate growth phenotype (Fig. 2). The two mutant *acuA* alleles encoding the AcuA^{R42H} and AcuA^{T169A} proteins were cloned into protein overexpression vector pTYB12, AcuA proteins were overproduced and isolated, and the wild-type AcuA (AcuA^{WT}) enzyme was isolated as a control using the same procedure. Gel filtration analysis of the AcuA^{WT} protein was consistent with the enzyme being a monomer (see Fig. S4A in the supplemental material).

Optimization of reaction conditions. We determined optimal conditions for AcuA$_{Bs}$ activity using as the substrate a synthetic peptide of AcsA from *B. subtilis* and Ac-CoA. The pH optimum was found to be 7.5, and the temperature optimum was 37°C (see Fig. S4B and C in the supplemental material). We could not test AcuA activity at temperatures above 37°C because the rate of spontaneous Ac-CoA cleavage was higher than the rate of consumption of Ac-CoA by AcuA. In addition, the spontaneous cleavage of Ac-CoA at temperatures above 37°C decreased the known concentration, and therefore, precise rate calculations were not possible. Increasing the ionic strength of the reaction mixture decreased the activity of AcuA (see Fig. S4D in the supplemental material).

Strong ionic interactions maintain AcuA$_{Bs}$ in its active conformation. In previous work, we noted the unusual heat stability of AcuA$_{Bs}$ (5). This feature of the enzyme was not understood, but it presented us with the challenge of finding a way of inactivating the enzyme. During the optimization of the assay conditions, we learned that the AcuA$_{Bs}$ activity was sensitive to salt concentration; however, a high concentration of KCl (500 mM) was needed to completely inactivate the enzyme (see Fig. S4D in the supplemental material). The predicted isoelectric point for AcuA$_{Bs}$ is 5.3, and it therefore harbors a net negative charge at pH 7.5, where activity was highest. The addition of KCl screens away ionic interactions of AcuA$_{Bs}$, decreasing its activity. This finding strongly suggests that the biologically active form of AcuA$_{Bs}$ is maintained by strong

ionic interactions. This new knowledge provides the means to efficiently terminate AcuA$_{Bs}$ reactions.

Kinetic analysis of AcuA^{WT} and variant AcuA enzymes. The rates of the reactions catalyzed by AcuA^{WT} and variant AcuA proteins as a function of substrate concentration were determined by using the graphing and statistical software package Prism v4 (GraphPad) (see Fig. S5 in the supplemental material). Under optimal assay conditions, the AcuA^{R42H} and AcuA^{T169A} variants had the same kinetic parameters but differed from the wild-type protein in their reduced K_m for Ac-CoA (two- to threefold lower than for AcuA^{WT}) and their reduced turnover number (threefold slower) (Table 1). Although the catalytic efficiency of the AcuA^{R42H} and AcuA^{T169A} variants was the same as that of the AcuA^{WT} protein, those proteins did not inhibit growth when overproduced, suggesting that they were unstable in vivo.

We probed whether or not the R42H and T169A mutations had a structural effect by assessing changes in the known heat stability of the AcuA enzyme (5). After heating AcuA^{WT} and variant AcuA proteins to 100°C for 30 min, the acetyltransferase activity of the enzyme was assayed in vitro. The AcuA^{R42H} protein retained 54% ± 11% of the activity of the wild-type enzyme treated under the same conditions, whereas the AcuA^{T169A} protein retained 60% ± 13% of the activity (data not shown).

The AcuA$_{Bs}$ protein is less responsive to low levels of Ac-CoA but more responsive to its peptide substrate than eukaryotic GNATs. AcuA$_{Bs}$ requires more Ac-CoA substrate to reach saturation than yeast GCN5 (yGCN5) and P/CAF (p300/CREB-binding-protein-associated factor) (22, 23). AcuA$_{Bs}$ was substantially less responsive to low levels of Ac-CoA, as shown by a K_m for Ac-CoA that is 1 order of magnitude higher

TABLE 1. Kinetic parameters of AcuA^{WT} and variant AcuA$_{Bs}$ enzymes

Protein	Peptide substrate				Ac-CoA substrate			
	K_m (mM)	V_{max} (mM min^{-1} mg^{-1})	k_{cat} (s^{-1})	k_{cat}/K_m (s^{-1} M^{-1})	K_m (mM)	V_{max} (mM min^{-1} mg^{-1})	k_{cat} (s^{-1})	k_{cat}/K_m (s^{-1} M^{-1})
AcuA^{WT}	20 ± 2	0.9 ± 0.02	0.3	1.5×10^4	22 ± 2	0.8 ± 0.03	0.3	1.4×10^4
AcuA$^{R42H a}$	37 ± 5	0.3 ± 0.01	0.1	2.7×10^3	8 ± 1	0.2 ± 0.01	0.1	1.3×10^4
AcuA$^{T169A a}$	37 ± 5	0.3 ± 0.01	0.1	2.7×10^3	9 ± 1	0.2 ± 0.01	0.1	1.1×10^4
yGCN5^b	490 ± 80		1.7 ± 0.1	3.5×10^3	2.5 ± 1.4			
P/CAF^c	532 ± 81		2.3 ± 0.07	4.3×10^3	0.98 ± 0.31			

[a] The peptide substrate was not used at saturating concentrations.
[b] Data previously published by others (23).
[c] Data previously published by others (22).

than that of yGCN5 and P/CAF (Table 1). In contrast, the K_m of AcuA$_{Bs}$ for its peptide substrate was 25-fold lower than that of yGCN5, suggesting that either *B. subtilis* synthesizes less AcsA or the activity of AcsA in this bacterium is very high and needs to be tightly controlled. The latter would be a plausible explanation given the deleterious effect that high levels of Acs have on cell growth (9; J. Garrity, S. R. Brinsmade, and J. Escalante-Semerena, unpublished results).

The explanation for the difference in K_m values between AcuA$_{Bs}$ and yGCN5 may lie in the intracellular concentration of the CoA pool in *B. subtilis*, which was estimated at 71 pmol/mg (dry weight) (3).

The sixfold-slower turnover of AcuA$_{Bs}$ relative to those of yGCN5 and P/CAF may be explained by the absence of physiological pressures for the evolution of a faster AcuA$_{Bs}$ enzyme in *B. subtilis*. It would be of interest to isolate faster variants of AcuA$_{Bs}$ to determine what effect such variants would have on *B. subtilis* physiology.

The decreased catalytic efficiency of the AcuA^{R42H} and AcuA^{T169A} enzymes explains the growth phenotype shown in Fig. 2B. That is, since the AcuA^{R42H} and AcuA^{T169A} proteins retained some enzymatic activity (~25%) (Table 1), acetyla-tion (i.e., inactivation) of the entire pool of Ac-CoA synthetase (AcsA) was not achieved, thus resulting only in impaired growth on low acetate, the conditions where AcsA was required.

On the other hand, the G187E mutation had such a severe effect on the activity of the enzyme that the *S. enterica* over-production variant AcuA^{G187E} grew as well as the control strain carrying an empty vector, suggesting that the G187E mutation either completely inactivated or completely destabilized AcuA. The H177P mutation resulted in a growth phenotype similar to the one caused by the G187E mutation.

Structural modeling using the *Exiguobacterium sibiricum* AcuA crystal structure. The crystal structure of AcuA from *Exiguobacterium sibiricum* (AcuA$_{Es}$) was recently solved (Fig. 3) (Protein Data Bank accession no. 2q04). AcuA$_{Bs}$ and AcuA$_{Es}$ share substantial end-to-end identity (62%) and similarity (76%) (see Fig. S6 in the supplemental material). Residues R42, T169, G187, and H177 are conserved in both proteins. We used the structure of the AcuA$_{Es}$ protein to visualize where the AcuA$_{Bs}$ residues changed by mutation would lie in three dimensions so that we could try to explain the changes in enzymatic activity.
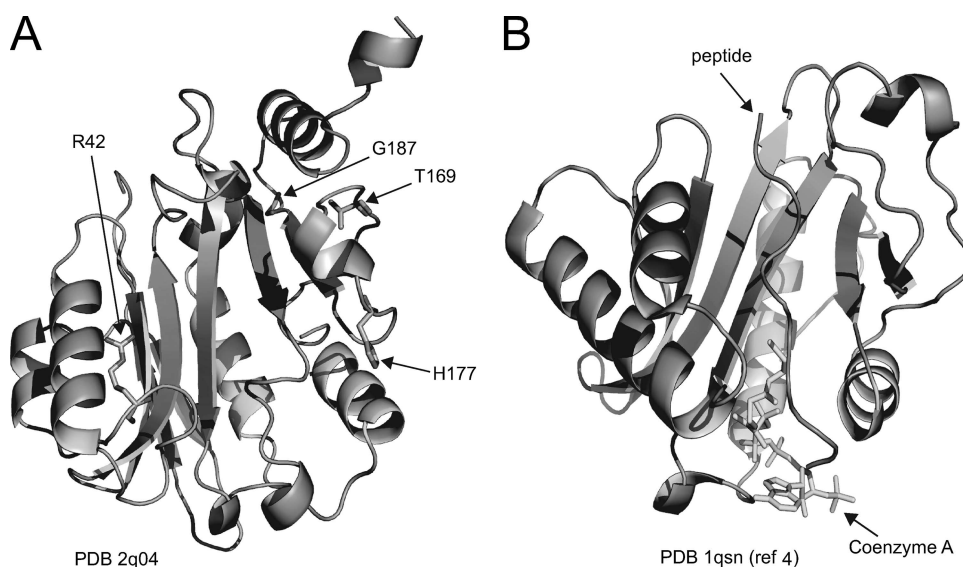

FIG. 3. Modeling AcuA$_{Bs}$ mutations into the structures of its homologs. (A) Reported structure of the bacterial apo-AcuA$_{Es}$. (B) Structure of *Tetrahymena* Gcn5 with substrates in the active site. This structure provides a point of reference for the location of the active site in AcuA$_{Es}$. PDB 2q04 and PDB 1qsn, Protein Data Bank accession numbers; ref, reference.

There are four characteristic motifs in GNATs, motifs A, B, C, and D (see Fig. S6 in the supplemental material). Residue R42 is part of motif C and is located before the α2 helix of the protein. We used the PyMOL software program (W. L. DeLano, the PyMOL molecular graphics system version 0.98) to introduce mutations into the AcuA$_{Es}$ structure, measured distances to neighboring side chain functions, and compared the distances to those found in the wild-type AcuA$_{Es}$ protein (see Fig. S7 in the supplemental material). These measurements are hypothetical and assume that no significant conformational change of the protein is caused by the mutation. In wild-type AcuA$_{Es}$, the imine N of the guanidinium group of R42 forms a salt bridge with the hydroxyl of the γ-carboxylate function of Q47, and these functions are 2.6 Å apart. We hypothesize that in the AcuA^{R42H} variant protein, this interaction is likely absent. Residue T169 is conserved in both proteins but is not part of any consensus GNAT motif; T169 is located after the β8 sheet of the AcuA$_{Es}$ protein. In the AcuA$_{Es}$ structure, the side chain hydroxyl group of T169 is 3.3 Å away from the peptide bond N of D171. This salt bridge is likely absent in the AcuA^{T169A} variant protein. Residue H177 is located immediately after the α10 helix of the protein. The carbonyl of H177 forms a salt bridge with the δN of N180 (2.9 Å). This ionic interaction may be present in the AcuA^{H177P} protein, but the negative effect of the mutation may arise from the proximity of the resulting vicinal prolyl side chains (P177 and P178). We suspect that such a change results in a loss of flexibility that could restrict conformational changes necessary for catalysis.

Residue G187 is part of hydrogen-bonded turn 12 of the protein after sheet β9 and before helix α11. In the AcuA^{G187E} protein, interactions between the γ-carboxylate group of Glu at position 187 with the peptide bond N atoms of residues H127 and M125 may form and restrict the flexibility of the enzyme to the point of rendering it completely inactive.

Variant proteins AcuA^{G187E} and AcuA^{H177P} could not be overproduced, as judged by sodium dodecyl sulfate-polyacrylamide gel electrophoresis (data not shown), suggesting that these variants are rapidly turned over by the cell.

GNAT motifs, structural considerations, and AcuA$_{Bs}$ activity. As shown in Fig. S6 in the supplemental material, AcuA$_{Bs}$ contains four consensus motifs found in GNATs. Briefly, motif A contains the β sheet that is the core of the GNAT domain, specifically β6, which is involved in binding both substrates; motif B contains a portion of the β9 sheet, which also is involved in binding Ac-CoA; motif C is the least conserved of the GNAT motifs, and it is involved in orienting the protein substrate; and motif D forms part of the β sheet core and, together with motif A, makes up half of the catalytic site (4, 12, 13).

Noteworthy is the observation that two of the mutated residues (T169 and H177) map outside motifs A, B, C, and D. The other two mutations that we isolated, namely the R42H and G187 mutations, were found in motifs C and B, respectively (see Fig. S6 in the supplemental material). We hypothesize that the G187 and H177P changes greatly disrupt the structure of AcuA$_{Bs}$. Using heat stability as a parameter of structural integrity, we assessed the activities of the AcuA^{R42H} and AcuA^{T169A} variant proteins and found that both of these variants lost about 50% of the wild-type activity. Based on these

results, we suggest that these residues have a structural role but that they may also be involved in substrate binding, an idea supported by our kinetic data (Table 1).

A potential role for the AcuA enzyme in *B. subtilis* physiology. Recently, temporal gene expression during spore germination and outgrowth was examined (8). In this study, the *acuA* gene was upregulated during the 80 to 100 min of spore germination and into the outgrowth phase. Detailed genetic analyses of *acuA* expression and the identification of additional protein substrates in *Bacillus subtilis* are needed to gain insights into the scope of the AcuA-mediated posttranslational regulation in this bacterium.

REFERENCES

1. **Barlev, N. A., L. Liu, N. H. Chehab, K. Mansfield, K. G. Harris, T. D. Halazonetis, and S. L. Berger.** 2001. Acetylation of p53 activates transcription through recruitment of coactivators/histone acetyltransferases. Mol. Cell **8:**1243–1254.
2. **Berkowitz, D., J. M. Hushon, H. J. Whitfield, Jr., J. Roth, and B. N. Ames.** 1968. Procedure for identifying nonsense mutations. J. Bacteriol. **96:**215–220.
3. **Chohnan, S., H. Furukawa, T. Fujio, H. Nishihara, and Y. Takamura.** 1997. Changes in the size and composition of intracellular pools of nonesterified coenzyme A and coenzyme A thioesters in aerobic and facultatively anaerobic bacteria. Appl. Environ. Microbiol. **63:**553–560.
4. **Dyda, F., D. C. Klein, and A. B. Hickman.** 2000. GCN5-related *N*-acetyltransferases: a structural overview. Annu. Rev. Biophys. Biomol. Struct. **29:**81–103.
5. **Gardner, J. G., F. J. Grundy, T. M. Henkin, and J. C. Escalante-Semerena.** 2006. Control of acetyl-coenzyme A synthetase (AcsA) activity by acetylation/deacetylation without NAD$^+$ involvement in *Bacillus subtilis*. J. Bacteriol. **188:**5460–5468.
6. **Garrity, J., J. G. Gardner, W. Hawse, C. Wolberger, and J. C. Escalante-Semerena.** 2007. *N*-Lysine propionylation controls the activity of propionyl-CoA synthetase. J. Biol. Chem. **282:**30239–30245.
7. **Hallows, W. C., S. Lee, and J. M. Denu.** 2006. Sirtuins deacetylate and activate mammalian acetyl-CoA synthetases. Proc. Natl. Acad. Sci. USA **103:**10230–10235.
8. **Keijser, B. J. F., A. Ter Beek, H. Rauwerda, F. Schuren, R. Montijn, H. van der Spek, and S. Brul.** 2007. Analysis of temporal gene expression during *Bacillus subtilis* spore germination and outgrowth. J. Bacteriol. **189:**3624–3634.
9. **Kumari, S., R. Tishel, M. Eisenbach, and A. J. Wolfe.** 1995. Cloning, characterization, and functional expression of *acs*, the gene which encodes acetyl coenzyme A synthetase in *Escherichia coli*. J. Bacteriol. **177:**2878–2886.
10. **LeDizet, M., and G. Piperno.** 1987. Identification of an acetylation site of *Chlamydomonas* alpha-tubulin. Proc. Natl. Acad. Sci. USA **84:**5720–5724.
11. **Marmorstein, R.** 2001. Protein modules that manipulate histone tails for chromatin regulation. Nat. Rev. Mol. Cell Biol. **2:**422–432.
12. **Marmorstein, R.** 2001. Structure of histone acetyltransferases. J. Mol. Biol. **311:**433–444.
13. **Marmorstein, R.** 2001. Structure of histone deacetylases: insights into substrate recognition and catalysis. Structure **9:**1127–1233.
14. **Marmorstein, R., and S. Y. Roth.** 2001. Histone acetyltransferases: function, structure, and catalysis. Curr. Opin. Genet. Dev. **11:**1555–1561.
15. **Polevoda, B., and F. Sherman.** 2002. The diversity of acetylated proteins. Genome Biol. **3:**reviews0006.1–reviews0006.6.
16. **Schwer, B., J. Bunkenborg, R. O. Verdin, J. S. Andersen, and E. Verdin.** 2006. Reversible lysine acetylation controls the activity of the mitochondrial enzyme acetyl-CoA synthetase 2. Proc. Natl. Acad. Sci. USA **103:**10224–10229.
17. **Starai, V. J., I. Celic, R. N. Cole, J. D. Boeke, and J. C. Escalante-Semerena.** 2002. Sir2-dependent activation of acetyl-CoA synthetase by deacetylation of active lysine. Science **298:**2390–2392.
18. **Starai, V. J., and J. C. Escalante-Semerena.** 2004. Acetyl-coenzyme A synthetase (AMP forming). Cell. Mol. Life Sci. **61:**2020–2030.
19. **Starai, V. J., and J. C. Escalante-Semerena.** 2004. Identification of the protein acetyltransferase (Pat) enzyme that acetylates acetyl-CoA synthetase in *Salmonella enterica*. J. Mol. Biol. **340:**1005–1012.
20. **Starai, V. J., H. Takahashi, J. D. Boeke, and J. C. Escalante-Semerena.** 2003. Short-chain fatty acid activation by acyl-coenzyme A synthetases requires SIR2 protein function in *Salmonella enterica* and *Saccharomyces cerevisiae*. Genetics **163:**545–555.
21. **Sternglanz, R., and H. Schindelin.** 1999. Structure and mechanism of action

of the histone acetyltransferase Gcn5 and similarity to other *N*-acetyltransferases. Proc. Natl. Acad. Sci. USA **96:**8807–8808.

22. **Tanner, K. G., M. R. Langer, and J. M. Denu.** 2000. Kinetic mechanism of human histone acetyltransferase P/CAF. Biochemistry **39:**11961–11969.

23. **Tanner, K. G., M. R. Langer, Y. Kim, and J. M. Denu.** 2000. Kinetic mechanism of the histone acetyltransferase GCN5 from yeast. J. Biol. Chem. **275:**22048–22055.

24. **Vetting, M. W., L. P. S. de Carvalho, M. Yu, S. S. Hegde, S. Magnet, S. L. Roderick, and J. S. Blanchard.** 2005. Structure and functions of the GNAT superfamily of acetyltransferases. Arch. Biochem. Biophys. **433:** 212–226.

25. **Wardleworth, B. N., R. J. M. Russell, S. D. Bell, G. L. Taylor, and M. F. White.** 2002. Structure of Alba: an archaeal chromatin protein modulated by acetylation. EMBO J. **21:**4654–4662.